J. exp. Biol. ***175****, 89–114 (1993)*
Printed in Great Britain © The Company of Biologists Limited 1993

THE EFFECTS OF NEUROTRANSMITTERS ON THE INTEGRATIVE PROPERTIES OF SPINAL NEURONS IN THE LAMPREY

L. E. MOORE and JAMES T. BUCHANAN*

Department of Physiology and Biophysics, University of Texas Medical Branch, Galveston, TX 77550 USA, and *Equipe de Neurobiologie, Neuropharmacologie Moléculaire et Ecotoxicologie, C.N.R.S., Université de Rennes I, 35042 Rennes Cedex , France*

Accepted 23 September 1992

Summary

1. The integrative behavior of lamprey central neurons was analyzed by white noise frequency domain methods and simulated with a minimal, non-linear neuronal model consisting of two voltage-dependent processes: (i) a depolarizing inwardly directed conductance carrying calcium and monovalent ions and (ii) a repolarizing outwardly directly conductance representing a generalized potassium conductance. In addition to normal properties, the effects of neurotransmitters were interpreted with the model. Specifically, *N*-methyl-D-aspartate (NMDA)-induced properties were simulated under conditions where the intrinsic voltage dependence of the potassium channels was constrained by properties of lamprey neurons. However, the NMDA channel kinetics were fixed by the single-channel properties of other neurons. The effects of focally applied neurotransmitters on the membrane properties of intact spinal cord neurons were quantitatively described with a reduced neuronal model that was also used to simulate transmitter-induced responses. In addition, transmitters were also released synaptically by KCl depolarization of projecting neurons.

2. Both synaptically released transmitters and focally applied putative excitatory or inhibitory transmitters directly applied to the spinal cord generally resulted in a decrease in the magnitude of the impedance function that was modeled by a decrease in membrane resistance (shunting effect).

3. Local application of the inhibitory neurotransmitters glycine or gamma-aminobutyric acid (GABA) led to small voltage responses when recorded near the resting potential. However, large decreases in the magnitude of the impedance function were observed in both current-clamp or voltage-clamp recording modes.

4. The excitatory amino acids quisqualate, kainate and glutamate evoked depolarizations in current clamp that activated intrinsic voltage-dependent conductances and obscured the direct effects of the transmitters. Under voltage-clamp conditions these transmitters caused a small decrease in the impedance magnitude that could be modeled by a shunt.

*Present address: Department of Biology, Marquette University, Milwaukee, WI 53233, USA.

Key words: model, locomotion, oscillation, pacemaker, lamprey, *Ichthyomyzon unicuspis.*

5. In contrast to the other excitatory amino acids, NMDA elicited large increases, rather than decreases, in both the magnitude and the phase lag of the impedance function. These changes were modeled by a negative conductance (a voltage-dependent conductance that produces an inward current).

6. The reduced neuron model provides an experimentally based description of the highly oscillatory and non-linear responses observed during NMDA activation of the spinal neurons involved in the pattern generation of locomotion. Simulations of sustained oscillatory behaviors consistent with experimental observations were carried out to illustrate the NMDA-induced integrative properties of central neurons. The overall effect of the potential responses brought about by excitatory or inhibitory neurotransmitters was shown to alter both intrinsic and ligand-gated voltage-dependent conductances at subthreshold levels and, therefore, required a non-linear description.

7. Simulations of both the non-linear properties of the reduced neuronal model and its voltage-dependent transfer functions show that a simplified system with only two relaxation terms is sufficient to account for the currently available experimental data on the lamprey spinal cord. The criteria used in this analysis are that both the single-cell electrophysiological data taken under voltage-clamp conditions and the current-clamp oscillatory behavior must be displayed by the model.

Introduction

The non-linearities of neural systems have usually been quantitatively analyzed with the voltage-clamp method (Hodgkin and Huxley, 1952) in order to measure relaxation processes at defined membrane potentials and, using linear kinetic models, to obtain rate constants that are functions of voltage. Thus, the classical Hodgkin–Huxley (HH) reconstruction of the non-linear action potential is based on essentially a linear kinetic analysis at fixed membrane potentials. Although Hodgkin and Huxley used a power function, this has been shown to be equivalent to linear sequential states where the rate constants are interrelated (Armstrong, 1969). The small signal transfer function (Mauro *et al.* 1970) method employed here is analogous to the standard analysis. However, voltage- or current-clamp steps have an additional small signal perturbation added to elicit relaxation responses that can unambiguously be described by a linear kinetic model. The basic reason for using small signals in combination with frequency domain methods rather than conventional approaches is to take into account more easily the voltage-dependent cable properties (Koch, 1984) in the quantitative description of single-cell neuronal membrane properties.

This paper focuses on the voltage-dependent integrative properties of *in situ* central neurons possessing their normal dendritic trees. Under these conditions, an evaluation of membrane properties requires an estimation of cable properties that can be expected to be highly non-linear. The voltage-dependent ionic conductances were estimated at different membrane potentials by a piece-wise linear kinetic analysis to obtain rate constants. The rate constants as a function of voltage were then used to solve differential equations describing the properties of the central neuron (Koch and Segev, 1989).

Frequency domain measurements (Marmarelis and Marmarelis, 1978) provide an estimate of the neuronal electrotonic structure (Moore and Christensen, 1985) and, as a

consequence, a way to evaluate neurotransmitter action. Frequency-dependent responses, such as synaptic potentials, are complex functions of both the cable structure of the neuron and the kinetic properties of the ion channels in the cell membrane. An estimate of the relative contributions of these factors can be obtained by realistic simulations using data obtained during transmitter application. Frequency domain data lend themselves to curve fitting using models of the neuron that allow estimation of the cable properties and conductance kinetics of the cell (Moore and Christensen, 1985; Moore *et al.* 1988). Furthermore, one can make impedance function measurements at different membrane potentials in the presence of different neurotransmitters to determine how these factors alter the integrative properties of the neuron during activity.

Previous studies applying frequency domain methods to lamprey spinal neurons have shown that central neurons have distinct impedance functions (Buchanan *et al.* 1992; Moore and Christensen, 1985; Moore *et al.* 1993) that are dependent on both membrane potential and the activation of transmitter receptors. For example, after the addition of *N*-methyl-D-aspartate (NMDA) to the bath, many neurons exhibit pronounced resonances that are strongly voltage dependent (Moore *et al.* 1993).

The present study extends these observations first by examining the effects of a variety of applied transmitters as well as endogenous transmitter release on the impedance functions of spinal neurons and, second, by simulations of data-based models of transmitter action. The effects of the excitatory amino acids, NMDA, glutamate, quisqualate and kainate were tested using local application from a pressure pipette, allowing comparison of control, test and recovery impedance functions. In addition, the effects of the inhibitory neurotransmitters glycine and GABA were examined.

This analysis provides an experimentally based description of the highly oscillatory (Grillner *et al.* 1981, 1986, 1987; Jahnsen and Llinàs, 1984; Llinàs and Yarom, 1986) and non-linear responses observed during NMDA activation of the spinal neurons involved in the pattern generation of locomotion (Grillner *et al.* 1991). Simulations of sustained oscillatory behaviors (Rasmussun *et al.* 1990*a*,*b*) are consistent with experimental observations and provide a realistic neuronal model of NMDA-induced integrative properties. In addition to NMDA, other non-NMDA glutamate agonists also elicit patterned responses of locomotion that depend on non-linear intrinsic voltage-dependent conductances. However, the direct actions of these agonists themselves were generally modelled as simple membrane shunts. In general, the overall effect of the potential responses brought about by excitatory or inhibitory neurotransmitters will alter the voltage-dependent conductances at subthreshold levels, both intrinsic and ligand-gated and, therefore, require a non-linear description.

Materials and methods

The experiments were carried out on 13 adult silver lampreys (*Ichthyomyzon unicuspis*) ranging in size from 25–35 cm. The animals were kept in an aerated, freshwater aquarium at 4°C. For dissection, the animals were first anesthetized by immersion in tricaine methanesulfonate (Sigma) ($100 mg\,l^{-1}$). A spinal cord–notochord preparation was used (Rovainen, 1974). The physiological solution for dissection and for

the experiments consisted of the following (in $mmol\,l^{-1}$): 91 NaCl, 2.1 KCl, 2.6 $CaCl_2$, 1.8 $MgCl_2$, 4 glucose, 20 $NaHCO_3$, and was bubbled with a 95% O_2, 5% CO_2 mixture. The experimental chamber contained 5ml of physiological solution and was perfused constantly at a rate of $3ml\,min^{-1}$ and kept at a temperature of 8–10°C. The study was performed on a total of 58 neurons: 16 motoneurons identified physiologically by their ventral root projections, 3 giant interneurons (cells in the caudal cord with axons projecting contralaterally and rostrally) and 3 edge cells (putative stretch receptors located at the edge of the cord), identified morphologically, and 36 unidentified neurons. Many of the unidentified neurons were probably motoneurons, but physiological identification was not possible because they were impaled after addition of $1\,\mu mol\,l^{-1}$ tetrodotoxin (TTX) to the perfusion bath. The resting membrane potentials of all the neurons studied ranged between −58mV and −91mV with a mean of −71±7.5mV (±S.D.).

For application of agonists, a pressure micropipette system was used. The agonists were prepared in physiological solution. A micropipette containing a microfilament was back-filled with an agonist solution and the tip was broken so that volumes of about 5–15nl were ejected with each pressure pulse. The tip of the pipette was then lowered to within 100 μm of the dorsal surface of the spinal cord above the soma of the neuron impaled with the intracellular microelectrode, and a pressure pulse was applied to eject the agonist. The concentrations of agonists (all obtained from Sigma) used in the pressure micropipettes were as follows: $2mmol\,l^{-1}$ gamma-aminobutyric acid (GABA), $0.5mmol\,l^{-1}$ glycine (GLY), $5mmol\,l^{-1}$ D-glutamate (GLU), $2mmol\,l^{-1}$ *N*-methyl-D-aspartate (NMDA), $0.05mmol\,l^{-1}$ quisqualate (QA) and $0.5mmol\,l^{-1}$ kainate (KA). Application of the agonists was carried out in the presence of $1\,\mu mol\,l^{-1}$ TTX (Sigma).

The intracellular microelectrodes were made from capillary glass containing a microfilament and were filled with $4mol\,l^{-1}$ potassium acetate. Resistances were typically 50–70 MΩ. The intracellular amplifier (Axoclamp 2A) allowed recording in bridge mode, discontinuous current-clamp mode or discontinuous single-electrode voltage-clamp mode. The impedance functions were measured with a sum-of-sines method. A low-amplitude sum-of-sines signals was injected into the cell body *via* an intracellular microelectrode. The response of the cell was measured and a fast Fourier transform (1024 points) performed to produce a complex spectrum. This spectrum was plotted as impedance magnitude and phase *versus* frequency regardless of whether the measurement was performed in current-clamp or voltage-clamp mode. The sum-of-sines technique has been described previously (Moore and Christensen, 1985).

Theoretical analysis

Measurements of impedance functions are a useful way of characterizing the integrative properties of neurons because they give a direct overall view of the frequency-dependent properties. The shape and size of a synaptic potential originating from a brief synaptic current somewhere on the neuron is a complex function of the location of the synapse, the cable structure of the neuron and the kinetic properties of the various ion channels distributed in the membrane. The impedance function, measured from the cell body, reflects these various contributing factors. Thus, the effect of some perturbation of

the cell, such as a change in membrane potential or the presence of a neurotransmitter, is apparent over a wide frequency band.

The impedance function of an isopotential sphere with no active, voltage-dependent conductances consists of a maximum impedance magnitude at low frequencies and a monotonic decrease in the impedance magnitude at higher frequencies as the capacitance shunts the membrane. The phase is zero at low frequencies and shows a progressive lag to -90°. Addition of dendrites to this model results in a downward inflection in the magnitude and phase at relatively high frequencies. The effects of active, voltage-dependent conductances depend on whether they are positive or negative. A positive conductance, such as the delayed rectifier potassium channel, can result in a resonance, the peak of which shifts to higher frequencies with depolarization. Typically, the magnitude of the low-frequency components is reduced owing to the addition of the positive conductance to the passive membrane resistance. The phase generally exhibits less phase lag and, if a resonance is present, this is apparent as a phase lead at lower frequencies and a zero crossing to a phase lag at the resonance frequency. A negative conductance, such as the voltage-dependent sodium channel, generally cancels some of the resting positive conductance, resulting in a net increase in the impedance magnitude. The phase shows an enhanced phase lag and can go completely out of phase to -180° (Moore *et al.* 1993).

The parameters obtained from the frequency domain analysis can be used to simulate potential responses similar to the Hodgkin–Huxley (HH) simulation of an action potential from voltage-clamp data taken at fixed membrane potentials. In this regard voltage-clamp frequency domain measurements need to be made at different steady-state potentials just as the HH step clamp analysis is made over a range of step voltage levels and not during different phases of an action potential. The voltage clamp essentially linearizes the neuron because the kinetic processes are mainly set by the membrane potential. Although, in principle, it is not possible to predict a non-linear response from a linear analysis, the hybrid 'piece-wise' linear analysis of HH gives the voltage dependency of the rate constants (see Fishman *et al.* 1977), which allows computation of non-linear behavior. Thus, linear kinetic data taken over different, but fixed, membrane potentials can be used to construct the highly non-linear action potential. The analyses performed here of non-linear oscillations are first piece-wise linear measurements over a range of potentials and then simulations of kinetic responses. These procedures allow the computation of non-linear oscillations from the linear kinetic analysis carried out at different membrane potentials, again analogous to the computation of an action potential.

The most significant component of the non-linear character of ionic conductance mechanisms was shown by Hodgkin and Huxley (1952) to be the voltage dependency of the rate constants. In their original paper, empirical exponential functions of voltages were used to describe the rate constants (values of α and β) that, in turn, provided a comprehensive representation of the dynamic behavior. The critical point of the voltage-clamp analysis was the estimation of the voltage dependence of the time constants [e.g. $\tau_n=1/(\alpha+\beta)$] and steady-state variables [e.g. $n_\infty=\alpha/(\alpha+\beta)$] to obtain values of α and β for each ionic species.

In a similar manner, frequency domain measurements at different membrane potentials

can be used to obtain the rate constants of neurons where a conventional space voltage clamp is not possible. The membrane model used in this analysis involved the minimum number of uniformly distributed channel types that could describe the data obtained. It is thus parsimonious with regard to the number of ionic species used, since different potassium channels have been lumped together to form a positive conductance. In addition, both sodium and calcium inward currents through the relatively non-specific NMDA-induced channel are formally treated as one current. Thus, the inward NMDA channel current is defined as:

$$\begin{aligned} I_N &= G_{Nmax} N (V - V_{NMDA}) \\ &= G_N (V - V_{NMDA}), \end{aligned} \tag{1}$$

where N is the NMDA kinetic state variable having a value between 0 and 1 with a steady-state value, N_∞, I_N is current through the NMDA channel lumped together as one current species, G_{Nmax} is the maximum NMDA-induced conductance, V is the membrane potential and V_{NMDA} is the reversal potential for the NMDA-induced current. Similarly, the outward current is:

$$\begin{aligned} I_K &= G_{Kmax} K (V - V_K) \\ &= G_K (V - V_K), \end{aligned} \tag{2}$$

where K is the NMDA-activated outward current state variable, G_{Kmax} is the maximum potassium conductance and V_K is the potassium equilibrium potential.

Since there are no experimental data from lamprey suggesting a delay in the turning on of the NMDA-induced currents, the kinetic variables, N and K, are not raised to a power as was empirically done for the variables of the Hodgkin–Huxley formalism. Non-NMDA-activated currents showed no voltage dependency and were modeled as an increase in leakage or shunt conductance, G_L. Although there are kinetics associated with non-NMDA channels, they are not applicable for the time ranges investigated in this paper.

As with the Hodgkin–Huxley formalism (Hodgkin and Huxley, 1952), the total current is:

$$I = G_N (V - V_{NMDA}) + G_K (V - V_K) + G_L (V - V_L) + C_m (dV/dt), \tag{3}$$

where G_L is a leakage or shunt conductance, V_L is its reversal potential and C_m is the membrane capacitance.

The basic reaction for the activation of the NMDA-induced ion channel (Jahr and Stevens 1987, 1990*a*,*b*) has been proposed (Ascher and Nowak, 1988) as:

$$R\mathrm{Mg} \underset{k_+[\mathrm{Mg}^{2+}]}{\overset{k_-}{\rightleftharpoons}} R$$

and

$$R \underset{\epsilon}{\overset{\sigma}{\rightleftharpoons}} R_o$$

where R_o is the resting state of the receptor, R represents the unblocked activated form of the receptor with NMDA bound to it, and RMg is the magnesium-blocked form of the

activated receptor (Nowak *et al.* 1984). The constants, ϵ and σ, are the rates for binding and unbinding of NMDA to its receptor.

Since the process R to R_o is slow relative to the magnesium blocking action, σ=0.17ms^{-1} and ϵ=0.0006ms^{-1} (Holmes and Levy, 1990), the voltage-dependent kinetics for the NMDA-induced currents can be given by (Ascher and Nowak, 1988; Hodgkin and Huxley, l952):

$$dN/dt = k_{-}(1 - N) - k_{+}[Mg^{2+}]N, \tag{4}$$

where k_{-} and $k_{+}[Mg^{2+}]$ are forward and reverse voltage-dependent rate constants for closed and open conducting states. The kinetics associated with NMDA binding are not treated in this analysis.

Similarly, the potassium system with the variable, K, was modelled with the rate equation:

$$dK/dt = \alpha(1-K) - \beta K. \tag{5}$$

Thus, these equations are analogous to the HH equations except that there are no power functions and no inactivation.

In order to illustrate how these expressions are used in the frequency domain, a concise derivation for the potassium system of equation 5 will be given and then generalized to multiple currents. Thus, at any given voltage-clamp potential, small signals are superimposed to give the linear impedance (Mauro *et al.* 1970) as follows:

$$\delta I = C_m d(\delta V)/dt + G_{Kmax}K_\infty \delta V + G_{Kmax}(V - V_K)\delta K\,, \tag{6}$$

where C_m is the membrane capacitance, $K_\infty[K_\infty=\alpha/(\alpha+\beta)]$ is the steady-state value of K at a specified voltage. Using an expression for $d(\delta K)/dt$ (Mauro *et al.* 1970) and defining $\alpha_V=d\alpha/dV$ and $\beta_V=d\beta/dV$, the membrane admittance (Y)is given by:

$$Y = \delta I/\delta V = jwC_m + G_{Kmax}K_\infty + G_{Kmax}(V - V_K)\tau_K\{\alpha_V - K_\infty(\alpha_V + \beta_V)\}/[1+jw\tau_K], \tag{7}$$

where j is $\sqrt{-1}$, f is frequency, τ_K is $1/(\alpha+\beta)$, the relaxation time constant, and $w=2\pi f$.

In general for multiple ionic conductances, the form of equation 7 can be expressed as:

$$Y_T = jwC_m + 1/R + \Sigma_i G_i/(1+jw\tau_i), \tag{8}$$

where Y_T is the total admittance, R is the membrane resistance, G_i is the amplitude of the ith relaxation process as in equation 7, and τ_i is the time constant of the ith conductance. It should be noted that G_i, as defined by the numerator of the last term of equation 7, is dependent explicitly on membrane potential, V, and is equal to zero if either $V=V_K$ or the rate constants are not voltage-dependent, i.e. α_V and β_V are zero. Under these latter conditions the membrane is a passive parallel resistance and capacitance (RC) circuit and consists of just the first two terms of equation 8. The passive membrane time constant is defined as RC when $G_i=0$ and R is the membrane resistance. For each ionic conductance, as given by equation 7, the term R of equation 8 will include both the passive resistance and the second term of equation 7, i.e. the steady-state conductance, $G_{Kmax}K_\infty$. Thus, equation 7 shows that K_∞ and τ_K values can be experimentally determined directly from the impedance data taken at different membrane potentials. In addition, it should be noted

that, in equation 7, $G_i=G_{Kmax}(V-V_K)\tau_K\alpha_V-K_\infty(\alpha_V+\beta_V)$, which is equivalent to $G_i=G_{Kmax}(V-V_K)dK_\infty/dV$. In general, $G_i=G_{i,max}(V-V_{eq})(dn_{i\infty}/dV)$, where $G_{i,max}$ is the maximum conductance of the ith channel, n_i is the associated kinetic state variable described by a kinetic equation of the form of equation 5 and $n_{i\infty}$ is its steady-state value. Thus, the steady-state conductance *versus* voltage relationship can be used to estimate both $n_{i\infty}$ and G_i.

Data analysis

A reduced neuron model consisting of eight equal compartments coupled to an isopotential soma was curve-fitted to the experimental data to obtain membrane parameters for both passive and active properties (Moore *et al.* 1988). The admittances of the soma and the eight dendritic compartments were given by equation 8, but the parameters of the dendritic compartments were scaled as described below. In addition, there was a resistance, R_s, connecting each compartment. The parameters determined by the experimental data are as follows: C_m and T_c, the soma capacitance and ratio of compartmental to soma capacitance; R_m, the frequency- and voltage-independent resistance of the soma; G_i and τ_i, the amplitude and time constant, respectively, of the frequency-dependent voltage-sensitive conductance; GI, the frequency-independent value of the activated conductances; and finally, R_s. The electrotonic length (L) was calculated from the square root of the ratio of the zero-frequency impedance of a dendritic compartment to R_s (see the legend to Fig. 2 in Moore and Christensen, 1985). The computed L uses the steady-state values of the active conductances.

Control impedance data were first fitted with only the passive parameters C_m, R_m, T_c and R_s. The impedance data obtained after transmitter application were then fitted by fixing all parameters except R_m. If the fit was not adequate, R_m was fixed at the control value and the data were fitted by introducing first one and then a second active conductance. Active conductances, positive and negative, were distributed homogeneously. As previously described (Moore *et al.* 1988), a positive conductance represents a voltage-dependent conductance that produces a positive outward current. Similarly, a negative conductance represents a voltage-dependent conductance that produces an inward current. Activation of the non-NMDA receptors and inhibitory receptors were modeled as a shunt on the normal membrane properties that were themselves generally modeled as two relaxation processes reflecting inherent voltage-dependent inward and outward conductances. During the several hours that some of the cells were impaled by the intracellular electrode, the resting passive parameters changed slightly. Therefore, the control impedance data were fitted again with passive parameters for each pair of control and test impedance data.

Results

Synaptic activity

To examine the effects of synaptic release of transmitter on the impedance functions of spinal neurons, neuronal activity was evoked by ejecting small volumes (approximately 10nl) of 200mmol l^{-1} KCl onto the surface of the spinal cord while making voltage-

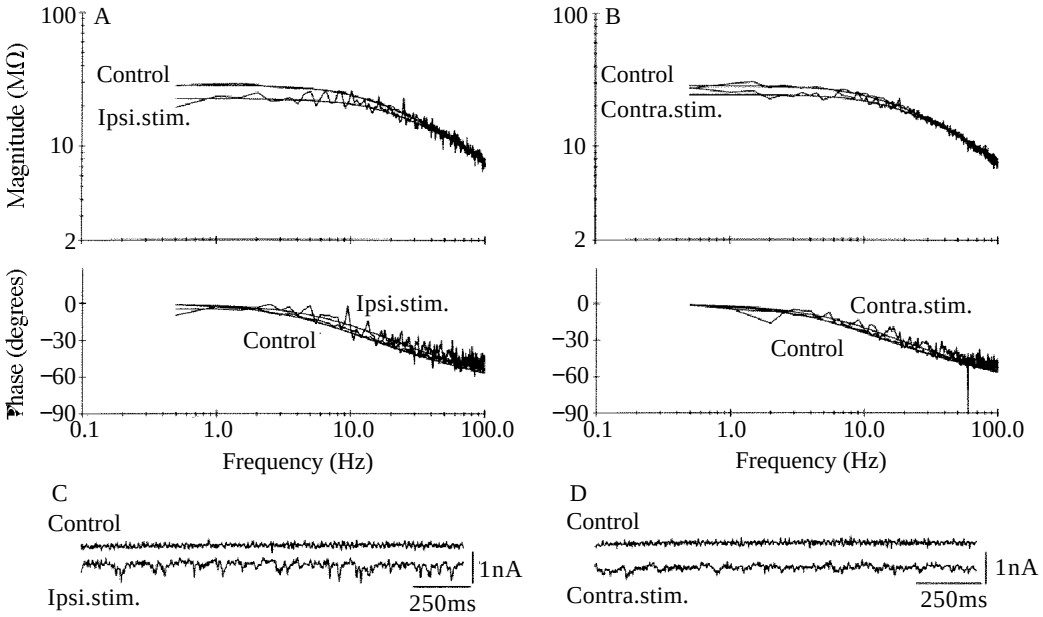

Fig. 1. The effect of endogenous transmitter release on the impedance function of a lamprey spinal neuron. The cell was recorded in single-electrode voltage-clamp mode (holding potential −86mV) in normal physiological solution. Small volumes of 200mmol l^{-1} KCl were ejected onto the ipsilateral (A) or contralateral (B) surface of the spinal cord several spinal segments rostral to the neuron and downstream in the perfusion flow. The KCl application caused neurons to fire action potentials for several seconds, and some of the activated neurons synapse directly or *via* interneurons upon the illustrated neuron. For the impedance plots, magnitude is placed above phase. The plots consist of lines connecting data points which themselves have been omitted. The smooth curve through the data lines is the fitted impedance function. Below the impedance functions are the currents recorded just prior to the sum-of-sines stimulus, before (control) and after application of the KCl. Model parameters: A, control: C_m=0.18nF, R_m=120 MΩ, T_c=1.1, R_s=9.3 MΩ, L=2.3; ipsilateral KCl: C_m=0.18nF, R_m=79 MΩ, T_c=1.1, R_s=9.3 MΩ, L=2.8; B, control: C_m=0.18nF; R_m=120 MΩ, T_c=1.1, R_s=9.3 MΩ, L=2.3; contralateral KCl: C_m=0.18nF, R_m=90 MΩ, T_c=1.1, R_s=9.3 MΩ, L=2.6. (C,D). Voltage-clamped synaptic currents measured before and after KCl application. Cell 80B31.

clamp impedance measurements from a single nerve cell. The site of KCl application was several spinal segments rostral to the recorded neuron and downstream in the bath perfusion flow. Therefore, the intracellularly recorded neuron received synaptic input resulting from the firing of neurons depolarized by the KCl in a localized region, but it was not directly exposed to the KCl. The KCl application could be restricted to either side of the cord. Ipsilateral KCl pulses tended to depolarize the recorded neuron and to cause firing of ipsilateral ventral roots for several seconds. Contralateral KCl pulses, in contrast, tended to hyperpolarize the recorded neurons and did not cause ventral root firing.

One or two seconds after the KCl application, the neuron reached a steady-state level of synaptic input (Fig. 1). The membrane potential of the illustrated neuron was clamped at −86mV, which was 20mV hyperpolarized with respect to the resting potential, in order

to prevent action potential firing. Therefore, both inhibitory and excitatory synaptic currents were in an inward direction. A sum-of-sines voltage-clamped signal was then applied to the cell *via* the intracellular electrode and the current response was measured. Both the magnitude and the phase of the impedance functions were affected by the synaptic activity: the magnitude decreased over a wide frequency range and the phase became less negative (less phase lag). Using an eight-compartment model neuron, the data were fitted by a passive (i.e. not voltage-dependent) decrease in the membrane resistance (by 33% for ipsilateral KCl and 23% for contralateral KCl). Fits with one or more active conductances were no better than the passive fits. Of 9 cells tested in this manner (including 4 motoneurons, 2 giant interneurons and 3 unidentified neurons), 7 showed responses similar to those in Fig. 1 while 2 cells showed only increased data scatter after ipsilateral KCl application but with no consistent change in the impedance function. Therefore, a generalized, non-specific, endogenous release of transmitter(s), whether predominantly excitatory or inhibitory, tends to cause a membrane shunt across a wide frequency range. The lack of an impedance decrease in some cells could be due to a simultaneous activation of NMDA and shunting non-NMDA receptors. It will be shown below that activation of NMDA receptors causes an impedance increase; thus, it is possible to balance out an impedance decrease and observe no net impedance change.

Neurotransmitter application

The specific effects of a single neurotransmitter were evaluated by direct application from a pressure pipette. By applying neurotransmitter agonists from a micropipette positioned about 100 μm above the surface of the spinal cord, it was possible to measure the change in the impedance properties produced by the agonist on the neuron compared to control measurements made just prior to agonist ejection. These experiments were carried out on the isolated spinal cord perfused with normal physiological solution containing $1\,\mu mol\,l^{-1}$ tetrodotoxin (TTX). Both current- and voltage-clamp measurements were made.

Application of either glycine ($0.5 mmol\,l^{-1}$) or GABA ($2 mmol\,l^{-1}$) produced little voltage or current response when recorded near resting potential. Under current-clamp conditions, the cells responded with either a hyperpolarizing or a depolarizing response, which is consistent with a reversal potential for these transmitters near the resting potential. The effects on the impedance functions, however, were much more dramatic. For example, in Fig. 2 the impedance functions for a cell recorded under current clamp before and after local application of glycine (Fig. 2A) and GABA (Fig. 2B) are shown. In these two cases there was a small (approximately 5mV) depolarization upon application of the agonist, and a large decrease in the magnitude and the phase lag of the impedance function. These changes in the impedance functions were fitted by a decrease in the passive membrane resistance: a 63% reduction for glycine and a 74% reduction for GABA (Fig. 2). Fits with one or two active conductances were no better than the passive fits. The magnitude of the effect of the agonists was a function of several factors, such as the concentration and volume of the agonist ejected, the perfusion speed and the distance

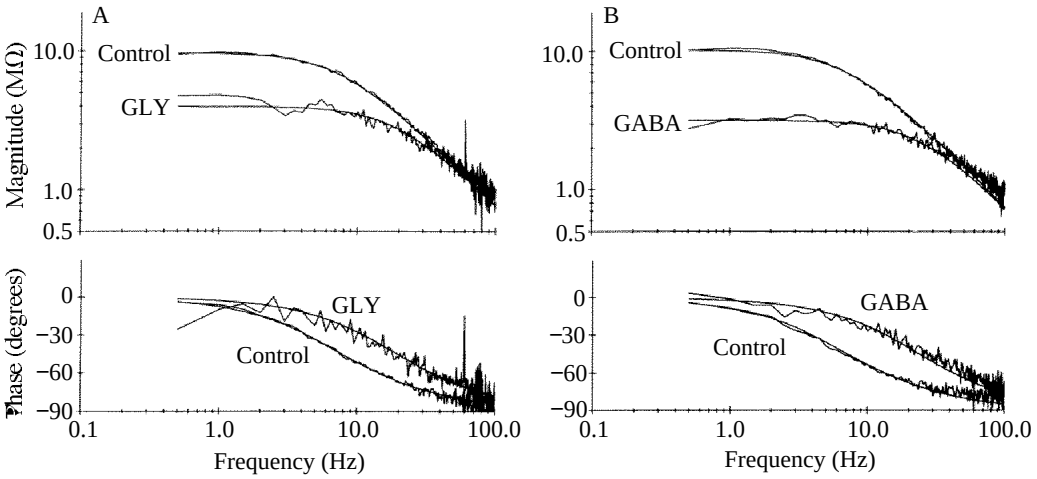

Fig. 2. The effect of inhibitory neurotransmitters on the impedance function of a motoneuron recorded in current-clamp mode. (A) Glycine (GLY) (0.5mmol l^{-1}) applied from a pressure pipette to the dorsal surface of the spinal cord above the soma. (B) Application of gamma-aminobutyric acid (GABA) (2mmol l^{-1}). 1 μmol l^{-1} TTX present in the bath. Model parameters. A, control: C_m=2.0nF, R_m=12 MΩ, T_c=0.17, R_s=15 MΩ, L=3.7; GLY: C_m=2.0nF, R_m=4.6 MΩ, T_c=0.17, R_s=15 MΩ, L=6.0; B, control: C_m=2.1nF, R_m=14 MΩ, T_c=0.44, R_s=21 MΩ, L=6.5; GABA: C_m=2.1nF, R_m=3.6 MΩ, T_c=0.44, R_s=21 MΩ, L=13. Cell 67B37.

of the pipette tip from the spinal cord. Therefore, the magnitude of the effects could vary from cell to cell.

Under voltage-clamp conditions, similar effects on impedance functions were observed, namely minimal current responses to the application of glycine and GABA (holding potential= −80mV), but a 40% reduction in membrane resistance for glycine and a 35% reduction for GABA. In total, 15 neurons were tested with glycine, including 5 motoneurons, 1 giant interneuron and 9 unidentified neurons; for GABA, 10 neurons were tested, including 5 motoneurons, 1 edge cell and 4 unidentified neurons. All cells tested showed changes in impedance similar to those illustrated in Fig. 2.

In addition to inhibitory transmitters, excitatory amino acids were pressure-ejected onto the surface of the spinal cord at concentrations required to evoke depolarizations of about 10mV. Current-clamp recorded impedance functions on one neuron are shown in Fig. 3, and the voltage-clamp recorded functions from a second neuron are shown in Fig. 4. Local application of quisqualate (0.05mmol l^{-1}) and kainate (0.5mmol l^{-1}) each caused a decrease in the magnitude of the impedance function with a gentle resonance around 3Hz (Fig. 3A,B). These data were best fitted with a combination of a negative and a positive conductance compared to a single positive conductance or a membrane shunt. For quisqualate, of 12 neurons tested in current clamp, including 3 motoneurons and 9 unidentified neurons, 9 cells exhibited similar changes in impedance to those illustrated. The remaining 3 cells showed no impedance change despite depolarizations of several millivolts. For kainate, of 10 cells tested in current clamp, including 4 motoneurons and 6

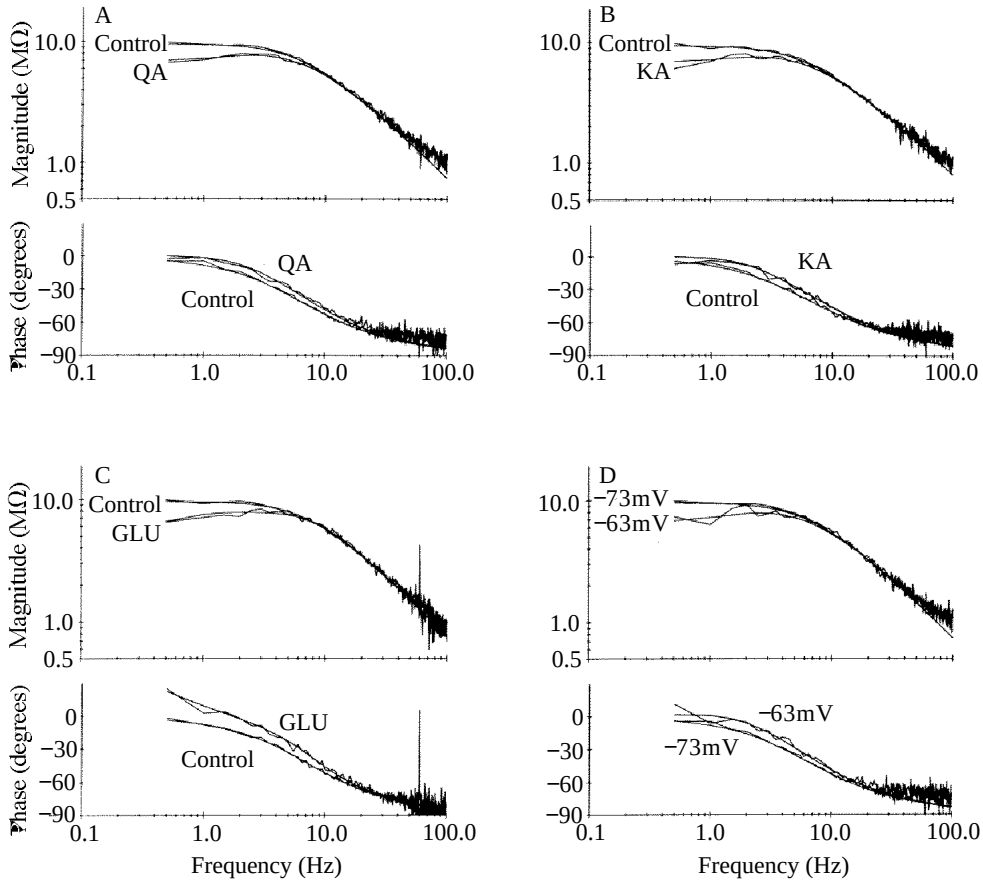

Fig. 3. Effects of excitatory amino acids on impedance functions recorded in current-clamp mode. (A) Quisqualate (QA) (0.05mmol l^{-1}). (B) Kainate (KA) (0.5mmol l^{-1}). (C) D-Glutamate (GLU) (5mmol l^{-1}). (D) Depolarization induced by current injection to a similar membrane potential produced by the agonists. 1 μmol l^{-1} TTX present in the bath. Model parameters. A, control: C_m=2.1nF, R_m=14 MΩ, T_c=0.19, R_s=9.7 MΩ, L=3.0; QA: C_m=2.1nF, R_m=14 MΩ, T_c=0.19, R_s=9.7 MΩ, G_1=−8.4nS; G_1 τ=0ms, G_2=23nS, G_2 τ=10ms, GI=7.7nS, L=3.4; B, control: C_m=1.9nF, R_m=16 MΩ, T_c=0.25, R_s=5.9 MΩ, L=2.4; KA: C_m=1.9nF, R_m=16 MΩ, T_c=0.25, R_s=5.9 MΩ, G_1=−24nS, G_1 τ=0ms, G_2=21nS, G_2 τ=90ms, GI=33nS, L=2.9; C, control: C_m=2.0nF, R_m=12 MΩ, T_c=0.17, R_s=15 MΩ, L=3.7; GLU: C_m=2.0nF, R_m=12 MΩ, T_c=0.17, R_s=15 MΩ, G_1=19nS, G_1 τ=20ms, G_2=320nS, G_2 τ=1700ms; GI=3nS, L=8.4; D, −73mV control: C_m=2.1nF, R_m=14 MΩ, T_c=0.19, R_s=9.7 MΩ, L=3.0; −63mV: C_m=2.1nF, R_m=14 MΩ, T_c=0.19, R_s=9.7 MΩ, G_1=-23nS, G_1 τ=0ms, G_2=29nS, G_2 τ=120ms, GI=34nS, L=3.7. Cell 67B37.

unidentified neurons, 8 cells showed similar changes to those illustrated and 2 cells were unaffected.

The response to glutamate (5mmol l^{-1}) in current clamp was also a decrease in the magnitude of the impedance function (Fig. 3C) with a broad resonance around 3Hz. These data were fitted with two positive conductances, one slow (τ=1.7s) and one fast (τ=20ms). All 8 neurons tested in current clamp, including 4 motoneurons and 4

unidentified neurons, showed similar changes in impedance functions. On some trials, however, 2 of these 8 neurons showed slight increases in the magnitude of the the impedance function, which would be consistent with an activation of NMDA receptors. This difference between glutamate *versus* quisqualate and kainate may be due to the simultaneous activation by glutamate of all three excitatory amino acid receptor subtypes, including NMDA receptors.

One complication in interpreting the current-clamp data is that these excitatory amino acids depolarize the neuron and this, in turn, could activate voltage-dependent channels in the membrane. Therefore, the decrease in the magnitude of the impedance function could either be due to the opening of transmitter-gated ion channels or to the depolarization alone, because the impedance functions of spinal neurons in lamprey have been shown to be sensitive to membrane potential (Moore and Buchanan, 1989; Moore and Christensen, 1985; Moore *et al.* 1993). To test whether membrane potential alone could account for the impedance changes observed in Fig. 3A,B,C, the neuron was depolarized by current injection through the intracellular electrode to a level similar to that elicited by the agonists (Fig. 3D). The depolarization alone produced a similar change in the impedance function to that of the agonists. In some neurons (7/15) it was clear that the impedance changes evoked by the agonist were greater than the depolarization alone, indicating that both factors, depolarization and opening of transmitter-gated channels, were contributing to the change. In the remaining neurons (8/15), the agonist caused either the same or a smaller impedance change than the depolarization alone.

To determine whether these excitatory amino acid agonists could have an effect on the impedance function regardless of membrane potential depolarization, the agonist applications were repeated on neurons during voltage clamp (Fig. 4). In this case, the application of agonist still resulted in a decrease in magnitude and phase lag, but data were fitted with a change in membrane resistance only without a requirement for active conductances. This analysis is consistent with the hypothesis that these particular neurons at their resting level did not have measurable active conductances and, furthermore, that there were no observable voltage-dependent processes elicited by the tested agonists if the potentials were voltage-clamped to their resting values. The data for the illustrated cases were fitted by a reduction in the membrane resistance (shunting effect): 11% for glutamate, 28% for kainate and 29% for quisqualate.

N-Methyl-D-aspartate (NMDA) had a very different effect on the membrane potential and impedance function of spinal neurons from the excitatory amino acid agonists discussed above. In normal physiological solution containing 1 μmol l^{-1} TTX, pressure-pulse applications of glutamate, quisqualate or kainate produced smooth depolarizations (Fig. 5A). NMDA (2mmol l^{-1}), however, evoked a depolarization which could develop into membrane potential oscillations (Fig. 5A). With regard to impedance functions, the non-NMDA agonists usually elicted a decreased magnitude (Fig. 4A,B,C), whereas NMDA generally elicited an increased magnitude (Figs 4D and 6). In the current-clamp recording of Fig. 6 the best fit of the data required both a relatively large negative and a positive conductance, such that the sum was a positive conductance whose net value was less than that recorded under resting conditions. The calculated d.c. electrotonic length of this cell decreased to 67% of the resting value in the presence of NMDA. In contrast to

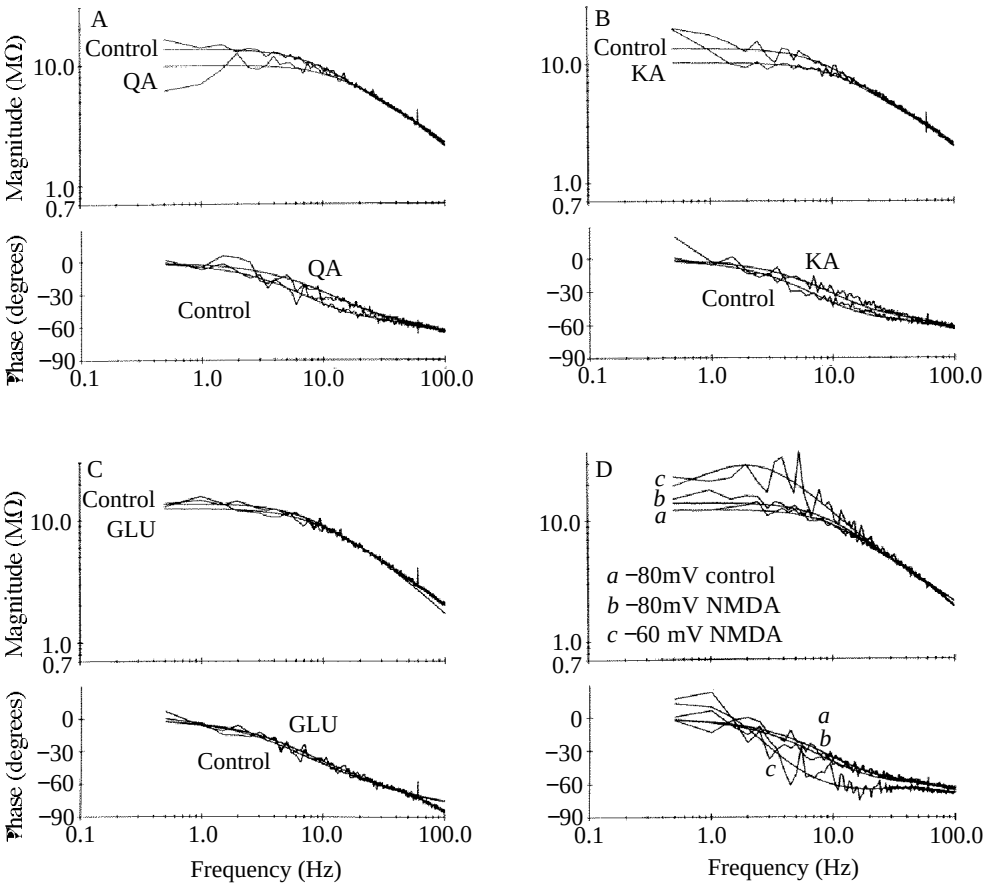

Fig. 4. The effects of excitatory amino acids on impedance functions recorded in voltage-clamp mode. (A) Quisqualate (QA) (0.05mmol l^{-1}). (B) Kainate (KA) (0.5mmol l^{-1}). (C) D-Glutamate (GLU) (5mmol l^{-1}). (D) *N*-Methyl-D-aspartate (NMDA) (2mmol l^{-1}). Voltage clamping at −60mV (*c*) gave a much larger response to NMDA than clamping at −80mV (*b*). Non-NMDA excitatory amino acids did not exhibit voltage dependence. 1 μmol l^{-1} TTX present in bath. Model parameters. A, control: C_m=0.47nF, R_m=37 MΩ, T_c=0.3, R_s=1.7 MΩ, L=0.93; QA: C_m=0.47nF, R_m=27 MΩ, T_c=0.3, R_s=1.7 MΩ, L=1.1; B, control: C_m=0.47nF, R_m=37 MΩ, T_c=0.29, R_s=1.5 MΩ, L=0.85; KA: C_m=0.47nF, R_m=27 MΩ, T_c=0.29, R_s=1.5 MΩ, L=1.0; C, control: C_m=0.81nF, R_m=27 MΩ, T_c=0.21, R_s=4.1 MΩ, L=1.4; GLU: C_m=0.81nF, R_m=24 MΩ, T_c=0.21, R_s=4.1 MΩ, L=1.5; D, control: C_m=0.51nF, R_m=29 MΩ, T_c=0.22, R_s=1.5 MΩ, L=0.84; −80mV NMDA: C_m=0.51nF, R_m=34 MΩ, T_c=0.22, R_s=1.5 MΩ, L=0.78; −60mV NMDA: C_m=0.51nF, R_m=29 MΩ, T_c=0.22, R_s=1.5 MΩ, G_1=−430nS, G_1 τ=0ms, G_2=13nS, G_2 τ=261ms, GI=410nS, τ_2=0.22ms, L=0.72. Cell 70B32.

current clamp, the voltage-clamp recording of Fig. 4D show that NMDA had only a small effect when the holding potential was near the resting level (−80mV). However, when depolarized from the holding level to −60mV, there was again a large increase in the magnitude of the impedance function. These data were best fitted with two active

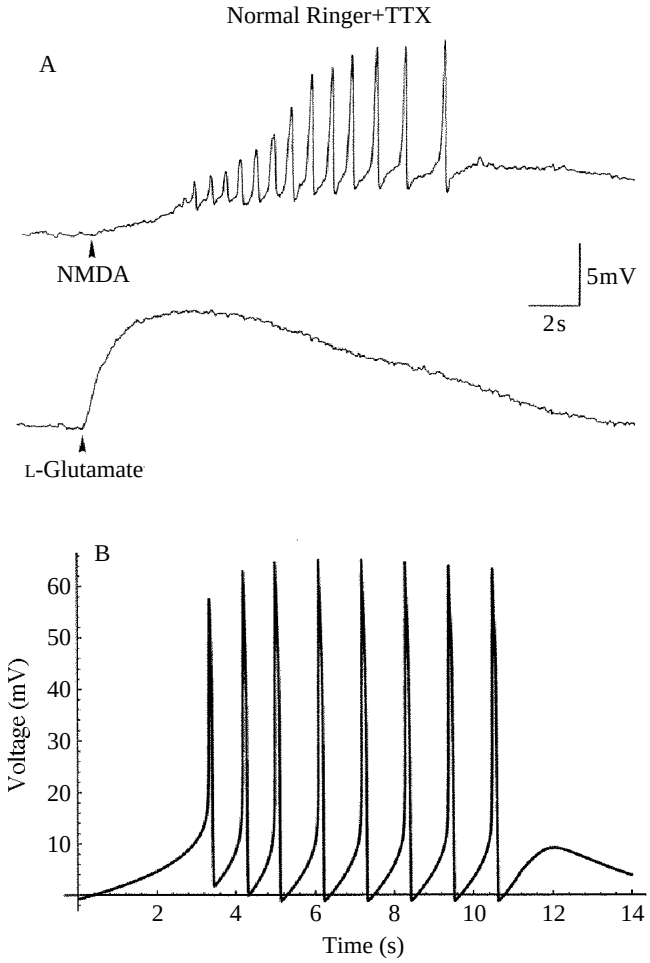

Fig. 5. (A) Membrane potential response *vs* time to local application of *N*-methyl-D-aspartate (NMDA) (top) and L-glutamate (bottom). The responses were recorded in current clamp in the presence of 1 μmol l^{-1} TTX. Cell 20G50. (B) Single compartmental simulation of a pressure pulse of NMDA using the equations and parameters discussed in the text except for G_{Nmax}, which was increased linearly in units of 0.0001mScm^{-2}ms^{-1} to a maximum of 0.5mScm^{-2}. See legend of Fig. 7 for values of standard parameters. At 11.2 s G_{Nmax} was decreased by the same rate to the end of the trace. The ordinate is millivolts of depolarization relative to the resting potential.

conductances, one negative and one positive. NMDA was tested on 23 neurons and showed effects similar to those described above in 17 of the 23 cells. These 17 cells included 5 motoneurons and 12 unidentified neurons. Five of the 23 neurons did not respond to NMDA; they were 1 motoneuron, 1 giant interneuron and 3 edge cells.

Reduced neuronal model simulations

The effects of excitatory transmitter action observed on lamprey neurons are of two distinct classes: (1) the induction of a relatively non-specific shunt that shows no intrinsic

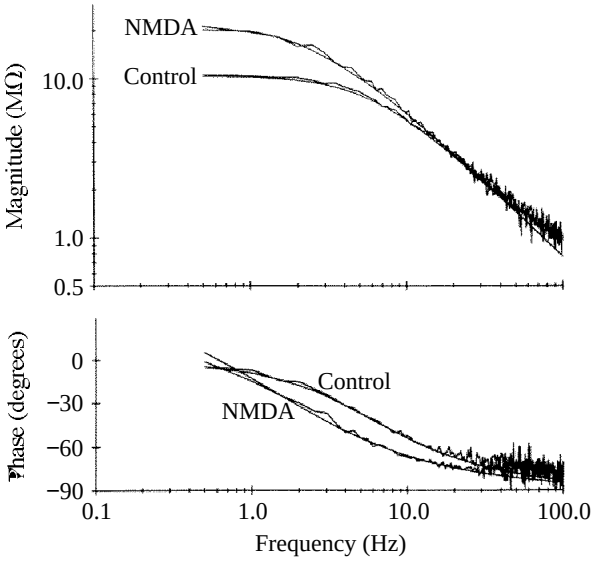

Fig. 6. The effect of *N*-methyl-D-aspartate (NMDA) (2mmol l^{-1}) on the impedance function recorded in current clamp. In contrast to the excitatory amino acids of Fig. 4, NMDA increased the magnitude and phase lag of the impedance function. 1 μmol l^{-1} TTX present in the bath. Model parameters. control: C_m=2.0nF, R_m=16 MΩ, T_c=0.22, R_s=9.0 MΩ, L=2.8; NMDA: C_m=2.0nF, R_m=16 MΩ, T_c=0.22, R_s=9.0 MΩ, G_1=−49nS, G_1 τ=0ms, G_2=14nS, G_2 τ=4.4ms, L=1.9. Cell 67B37.

voltage dependency, and (2) an activation of highly voltage-dependent conductances. The latter generally includes both the ligand-induced channels and intrinsic voltage-dependent processes associated with action potentials. The simulations presented here indicate how these two classes can interact and lead to the oscillatory behavior observed in lamprey neurons.

Numerous models exhibiting pacemaker behavior have been developed (Noble, 1966; see Rasmusson *et al.* 1990*a*,*b*). Recently, a modified Hodgkin–Huxley model containing a large number of ionic channels (Grillner *et al.* 1988; Brodin *et al.* 1991) was shown to exhibit behavior characteristic of that induced by NMDA (Wallén and Grillner, 1987). In contrast, the approach adopted in this paper is to develop a minimal model whose behavior at the single cell level is consistent with both voltage-clamped experimental data and the non-linear oscillations observed in TTX-treated spinal cords. The frequency domain data provide the relevant voltage-dependent membrane properties and thus an experimental basis for the model equations that can be used to predict complex non-linear behavior.

During NMDA activation of locomotion, at least four ionic channels (Hill *et al*. 1989; Brodin *et al.* 1991; Ekeberg *et al.* 1991) play important roles: the NMDA-activated channel carrying both sodium and calcium ions, a calcium-activated potassium channel (Hill *et al.* 1985) greatly enhanced by the increased calcium build-up *via* the NMDA channel, the voltage-dependent calcium channel, and the normal delayed potassium channel. Although four or more channels are present, the principal determinants of

NMDA oscillations can be reduced to two, one inward and one outward conductance. In the analysis of the frequency domain data, kinetic parameters for two ion channel types have been estimated over a range of membrane potentials that include those traversed during the locomotion cycle up to the threshold levels for action potential generation. The kinetic parameters for each relaxation process were estimated using a modified Hodgkin–Huxley formula having two voltage-dependent variables, N and K (see Morris and Lecar, 1981; Traub, 1982). The experimental parameters for each variable, N and K described above, were estimated from the frequency domain data at different membrane potentials. The maximum conductances, $G_{\mathrm{Nmax}}=0.5\mathrm{mS\,cm^{-2}}$ and $G_{\mathrm{Kmax}}=1.0\mathrm{mS\,cm^{-2}}$, were chosen to give impedance functions consistent with the experimental data as discussed below.

Both k_- and k_+ of equation 4 are voltage-dependent and have been fixed by single-channel NMDA data (Ascher and Nowak, 1988), as follows:

$$k_- = 5.4\exp(V/47) \tag{9}$$

$$k_+ = 0.61[\mathrm{Mg}^{2+}]\exp(-V/17)\,, \tag{10}$$

where the standard value of $[\mathrm{Mg}^{2+}]$ is $1.8\mathrm{mmol\,l^{-1}}$ and V is the membrane potential. k_- has units of $\mathrm{ms^{-1}}$; k_+ has units of $(\mathrm{mmol\,l^{-1}})^{-1}\,\mathrm{ms^{-1}}$.

The voltage-clamp frequency domain data provide estimates of membrane parameters at different potentials that allow the construction of a functional relationship between the rate constants and membrane potential. Since the values of k_- and k_+ are pre-determined, the only free values for voltage-dependent kinetic parameters are those of the outward conductances system, namely, α and β. The experimental findings that the outward conductance had a time constant in the second range and the dependence of resonant frequency on membrane potential provided constraints for the construction of the following equations:

$$\alpha = 2.3\times10^{-3}\exp(V/12), \tag{11}$$

$$\beta = 4.7\times10^{-4}\exp(-V/80). \tag{12}$$

Both α and β have units of $\mathrm{ms^{-1}}$.

These coefficients determine the values of the time constants and an asymmetry in the voltage dependence that is required to simulate the experimental finding of a resonance peak over a narrow range of potentials. Equations 9–12 allow a complete solution to equation 3 that forms the basic non-linear membrane model used in the simulations shown below. The properties of this model can be characterized in two modes: (1) the computed potential response to a variety of experimental conditions such as current injection (Frankenhaeuser and Huxley, 1964; MacGregor, 1987), NMDA concentrations and magnesium ion concentrations; and (2) the piece-wise linear formulation of equation 8 to simulate frequency domain functions that can be directly compared with the experimental data.

Simulation of frequency domain behavior

In order to relate the data obtained in the frequency domain and the properties of the

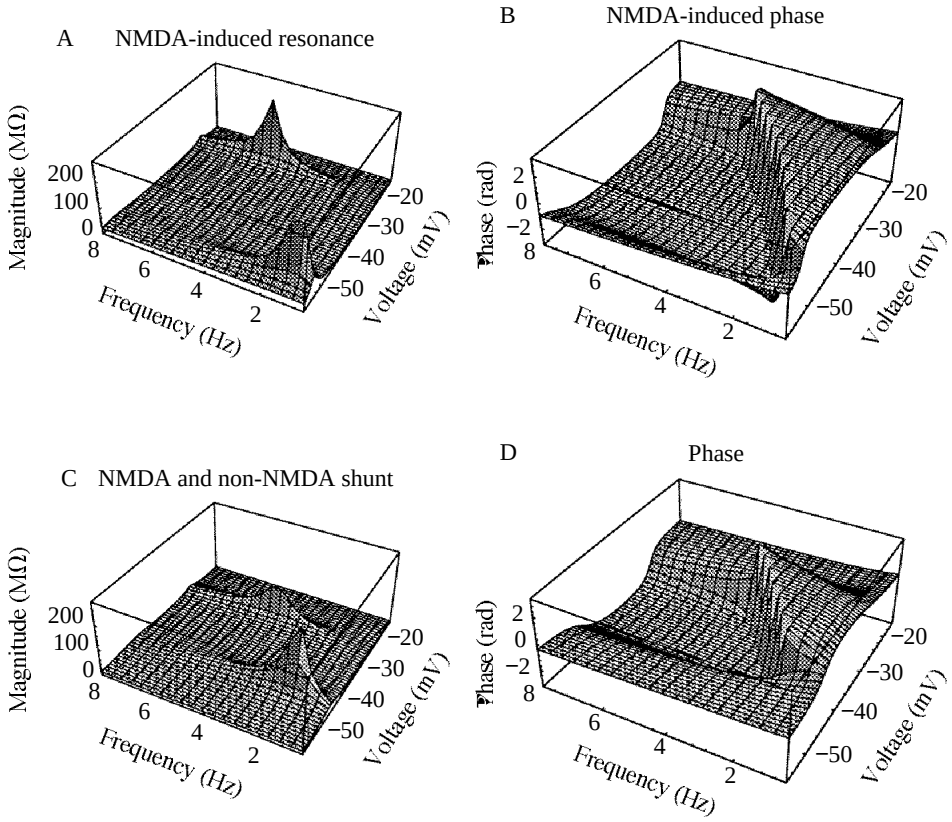

Fig. 7. (A and B) NMDA-induced resonance. Impedances were computed using equation 8 over a range of potentials from −70mV to −15mV each over a frequency range of 0.16–10.24Hz. The following values were used in the simulations unless otherwise indicated: C_m=1 μF cm^{-2}; G_L=0.2mScm^{-2}; V_L=−60mV; V_{NMDA}=55mV; V_K=−72mV; G_{Nmax}= 0.5mScm^{-2}; G_{Kmax}=1.0mScm^{-2}. Two peaks in the impedance magnitude are illustrated in the three-dimensional plot. The low-frequency peak observed at approximately 1Hz near V=−50mV represents the region of impedance enhancement. (C and D) A simulation of the effect of an additional shunt for non-NMDA receptor activation. The parameters are identical to those of A and B except that G_L=0.3mScm^{-2}. The higher-frequency resonance of about 5 Hz at approximately −25mV is typical of depolarized results observed during bath-application of NMDA and is in the range of the frequency of pacemaker oscillations observed under these conditions with TTX in the bathing solution.

reduced neuron model, impedances of the soma compartment were computed using equation 8 with the above functions for the rate constants (equations 9–12) and two relaxation terms (i.e. i=2). Over a range of potentials from −70 to −15mV, two peaks in the impedance magnitude are illustrated in the three-dimensional plot of Fig. 7A. The low-frequency peak observed around 1Hz near E=−50mV represents the region of impedance enhancement seen in Figs 4 and 6. Typically, the falling off of the peak at low frequencies is not seen, since its observation requires an extremely low-frequency band of measurement. These impedance functions illustrate a typical finding that, at moderate

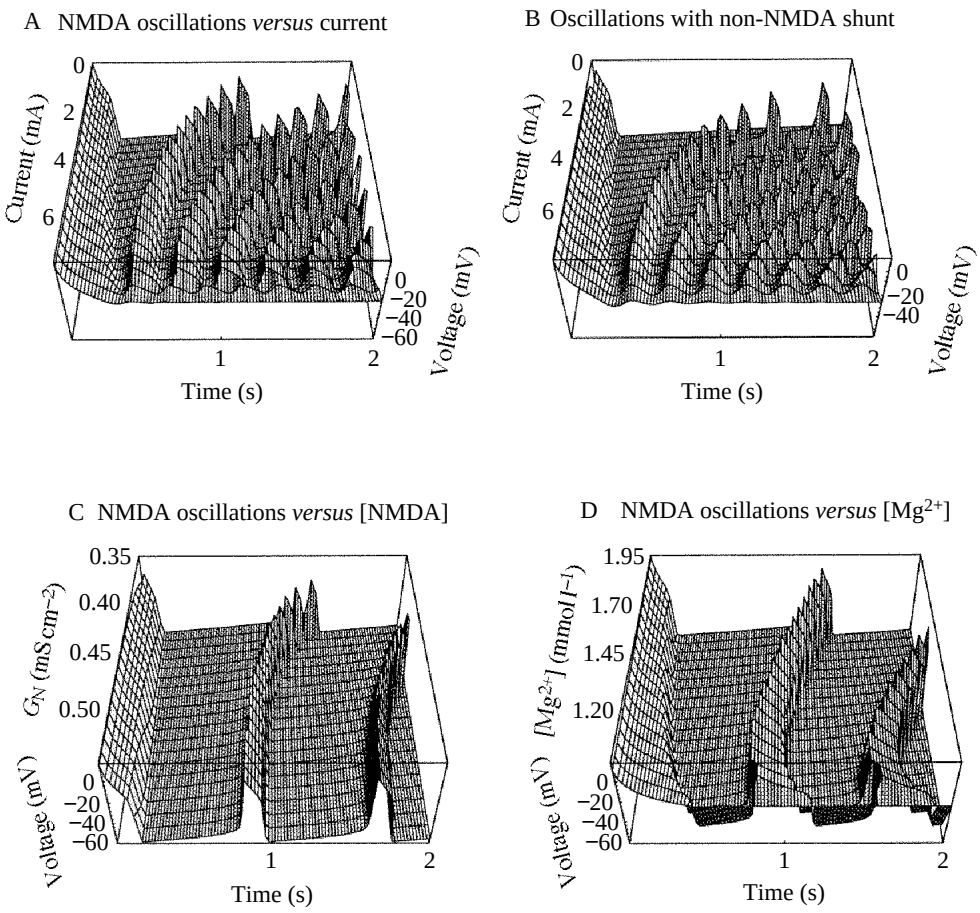

Fig. 8. (A and B) Simulations of the non-linear oscillations as a function of steady-state current levels are illustrated (range of current: 0–8mAcm^{-2}). These simulations are the non-linear solutions of equation 3 using the definitions of equations 9–12 and the parameters given in Fig. 7. Note that the oscillations in B are with an increased shunt of G_L=0.3mScm^{-2} The relative duration of the plateau phase of the potential oscillations decreases as the frequency decreases, which is consistent with experimental observation (Wallén and Grillner, 1987). The ordinate is mV of depolarization relative to the resting potential. (C) Dose–response behavior for NMDA activation is simulated and is similar to the dose–response behavior observed for fictive locomotion during NMDA perfusion (Brodin and Grillner, 1986). The range of maximal G_N values was 0.55–0.35mScm^{-2}. The ordinate is mV of depolarization relative to the resting potential. (D) The dependency of the oscillations on Mg^{2+} concentration is shown (range 1.0–1.95mmol l^{-1}); the oscillations increase in frequency with lower Mg^{2+} levels to a limit at which oscillations cease. At this point if the NMDA level of activation is reduced the oscillations return. This simulation result is similar to the experimental observation that lower levels of NMDA induce fictive locomotion when the Mg^{2+} concentration is reduced (see Brodin *et al.* 1991). The ordinate is mV of depolarization relative to the resting potential.

levels of depolarization when the negative conductance is just being activated, the impedance first increases and then decreases with further depolarization as the net conductance becomes negative. The initial increase is due to a reduction in the net conductance as the negative and leakage conductances sum algebraically. The higher-frequency resonance (Fig. 7A,C) of 4–5Hz with larger depolarizations is typical of results observed during bath-application of NMDA (Moore *et al.* 1993). The frequency of oscillations observed under these conditions with TTX in the bathing solution (see Fig. 5) is between the two resonant peaks depending on the level of injected current (see below).

An indication of the unstable potential region is seen in the phase functions of Fig. 7B,D, which correspond to Fig. 7A,C. As is characteristic of negative conductances (Moore *et al.* 1988) the phase approaches and can exceed 180° (2π rad). The discontinuity shown in these plots occurs precisely at the frequency at which the phase crosses 180°. The 180° crossing occurs at higher frequencies the greater the depolarization over a restricted potential range that coincides with the potential range between the two resonant peaks of Fig. 7A,C.

In order to simulate the mixed activation of NMDA and non-NMDA receptors by glutamate, the leakage conductance used in Fig. 7A,B was increased from its standard value of 0.2mmhocm^{-2} to 0.3mmhocm^{-2}. Fig. 7C,D shows that the increased shunt reduces the potential range of the region between the resonant peaks as well as that of the 180° crossing.

Simulations of non-linear oscillations

When solved by numerical methods (MacGregor, 1987), the reduced neuronal model (equations 3, 9–12) exhibits sustained non-linear membrane potential oscillations. Fig. 8A,B illustrates the dependence of the oscillations on steady-state current levels. The relative duration of the plateau phase of the potential oscillations decreases as the frequency decreases, which is consistent with experimental observation (Wallén and Grillner, 1987). At the higher levels of current, the oscillations eventually fuse and cease at a depolarized level. Oscillations simulated with an increased shunt, as in Fig. 7C,D, are shown in Fig. 8B to be only slightly decreased in frequency compared with the NMDA-induced oscillations of Fig. 8A, where the leakage conductance was normal. Increases in the leakage conductance above 0.35mmhocm^{-2} totally abolished the oscillatory behavior. This simulation result is consistent with the observation that there was no oscillatory behavior in the presence of glutamate or kainate and TTX (see Fig. 5A). Thus, although bath-applied glutamate activates NMDA receptors, the simultaneous activation of shunting non-NMDA sites prevents membrane oscillatory responses.

Similarly, dose–response behavior for NMDA activation is simulated in Fig. 8C and is similar to that observed for fictive locomotion during NMDA perfusion (Ault *et al.* 1980; Brodin and Grillner, 1986). Fig. 5B is a simulation of a pressure pulse of NMDA that was modeled as a linear increase and decrease of G_{Nmax}, the NMDA-activated conductance (equation 1), to account for diffusion delays.

Finally, the dependency of the oscillations on Mg^{2+} concentration is shown in Fig. 8D. The oscillations increase in frequency with lower Mg^{2+} levels, showing a markedly increased plateau duration to a limit at which oscillations cease and the membrane

remains depolarized. At this point, the oscillations return if the NMDA level of activation is reduced. This simulation result is similar to the experimental observation that lower levels of NMDA induce fictive locomotion when the Mg^{2+} concentration is reduced (see Brodin *et al.* 1991). In conclusion, a simple model of NMDA activation involving two voltage-dependent conductances, one inward and the other outward, appears to be sufficient to describe not only the impedance data but also a range of non-linear oscillatory behavior.

Discussion

The lamprey central nervous system is a convenient preparation for investigating the organization of motor control in vertebrates. In the study of the origin and control of locomotion, progress has been made identifying several classes of spinal interneurons that participate in swimming activity (Buchanan, 1986; Buchanan *et al.* 1989*b*; Buchanan and Grillner, 1987). Understanding how networks of nerve cells produce organized behavior requires knowledge at several levels: the integrative membrane properties of the neurons, the information-transfer characteristics of their synapses and the patterns of synaptic connectivity among the neurons (Getting, 1989).

Current–voltage responses of acutely isolated lamprey spinal neurons (Buchanan *et al.* 1989*a*) and intact *in vitro* lamprey spinal neurons (Moore *et al.* 1987) reveal that, in the presence of NMDA, as in neurons of the mammalian central nervous system (Mayer and Westbrook, 1985, 1987; Flatman *et al.* 1983), there is a region of negative slope conductance. Consistent with this finding, the results presented here demonstrate a dramatic difference between NMDA receptor activation and non-NMDA activation on the impedance properties of lamprey spinal neurons: NMDA causes the magnitude and phase lag of the impedance function to increase; kainate and quisqualate cause a decrease. Taken alone, such differences would imply differences in signal processing of the neuron depending upon whether it was being excited predominantly by NMDA or by non-NMDA receptors: NMDA activation tends to make the neuron more electrotonically compact while non-NMDA activation tends to have the opposite effect.

The transmitter released endogenously is unknown, but glutamate is a candidate (Brodin *et al.* 1988). Glutamate has been shown to be an effective agonist at all three excitatory amino acid receptor subtypes in other species (Watkins and Olverman, 1987). The ultimate action of the endogenous transmitter may therefore depend upon the relative activation of NMDA *versus* non-NMDA receptors at a particular synapse. There is some evidence in lamprey that synapses may be purely NMDA or purely non-NMDA or mixed (Dale and Grillner, 1986). The predominantly NMDA synapses would presumably result in enhancement of impedance, and the non-NMDA ones in a decrease in impedance at the synaptic site. Some evidence of mixed effects by glutamate were observed here. Glutamate tended to have less effect on impedance functions in spite of causing substantial depolarization and inward currents. This would be consistent with a cancellation of the negative conductance produced by NMDA receptor activation by the positive conductance of non-NMDA receptor activation. Also, in some instances, glutamate caused an increase in impedance, suggesting a predominance of NMDA

effects. Consistent with the mixed NMDA and non-NMDA activation, the endogenous release of transmitter sometimes caused strong currents and firing of ventral roots with no significant change in the impedance function. If glutamate is present in the extracellular space at low concentrations, as has been suggested (Sah *et al.* 1989), then NMDA receptors may be selectively activated in a uniform manner over large portions of the cell. Under these circumstances, such as might occur during swimming, the impedance and, hence, integrative properties of the neurons would be significantly altered.

One functional role of NMDA receptors could be to balance impedance effects of the non-NMDA excitatory receptors so that the neurons remain relatively constant in electrotonic length during excitation. However, if synapses are specialized as NMDA, non-NMDA or mixed, the local processing effects on the dendrites becomes considerably more complicated. In this regard, the presence of the two resonant peaks shown in Fig. 7 suggests that NMDA induces first an impedance enhancement at very low frequencies (in the second range) near the resting potential, leading to an enhancement of synaptic potentials to reach a membrane potential level that is unstable and eventually shows oscillatory behavior in the frequency range of a few Hertz, which is characteristic of the normal rhythmic behavior of the locomotor neurons. In addition, there are other mechanisms for maintaining the electrotonic length of the cell in the face of non-NMDA channel opening and depolarization. Most notably, any negative conductance channel will have a similar effect to NMDA. In normal physiological solution, depolarization of lamprey neurons alone can increase impedance magnitude as a result the activation of a TTX-sensitive steady-state negative conductance (Moore and Buchanan, 1989; Buchanan *et al.* 1992).

The membrane shunt produced by glycine and GABA, in contrast, is functionally consistent with their inhibitory effects. These transmitters inhibit the neuron in two ways: (1) they clamp the membrane below threshold at the equilibrium potential for chloride and (2) they shunt excitatory input. The endogenous release of transmitter evoked by KCl application to the contralateral side of the spinal cord always produced a clear shunt of the membrane, which is consistent with the effects of glycine and GABA. The shunt also confirms previous observations regarding the effects of glycine and GABA (Homma and Rovainen, 1978; Martin *et al.* 1970).

For the most part, the changes in impedance functions evoked by exogenous or endogenous transmitters demonstrate that transmitter action tends to cause a shunt of the membrane across a wide frequency band. An exception is NMDA activation, which can counter the shunting effect of kainate and quisqualate receptors. Typically, curve fits of NMDA required two conductances – one fast negative conductance and a slow positive conductance. The negative conductance was modeled with kinetics of the NMDA channel while the positive conductance was described as a potassium conductance. The latter is probably a combination of the delayed rectifier and the Ca^{2+}-dependent potassium channel (Grillner and Wallén, 1985).

The membrane property of a negative conductance, such as that induced by NMDA, can lead to impulse or synaptic potentials that are greatly enhanced (Holmes and Levy, 1990; Brodin *et al.* 1991), oscillatory or unstable, depending on the initial membrane potential. These effects, in conjunction with the pronounced resonance or tuning

characteristics of the synaptic transfer function, will lead to highly non-linear activation functions in the network simulations. One possibility is an individual synapse that increases its short-term response with use, i.e. increases its efficacy as the overall total synaptic input increases, thereby depolarizing the membrane and opening the NMDA-related channel. In addition to the NMDA effects, other, perhaps equally important use-dependent behavior, could come from either intrinsic membrane properties or those induced by other excitatory or inhibitory transmitters.

The simulations of Fig. 8 are consistent with experimental results that have shown that the frequency of stable NMDA-induced oscillations increases with a depolarizing current, decreased Mg^{2+} concentration and increased G_{Nmax} (NMDA receptor activation). The value of G_{Nmax} is proportional to the NMDA concentration in the model. In addition, at low Mg^{2+} concentrations, and consistent with experimental observations, simulated pacemaker oscillations are seen with lower values of G_{Nmax} than are equired at normal Mg^{2+} levels. Furthermore, both simulations and experiments show an increased magnitude of the oscillations with a reduction in G_K. Also, the shape of the non-linear waveform with the plateau phase is consistent with observations (Wallén and Grillner, 1987; Moore *et al.* 1987, 1993).

These simulations illustrate how frequency domain data can be used to construct non-linear differential equation models for comparison with neuronal behavior. Such a comparison can be used for parameter estimation in addition to the direct curve-fitting of voltage-clamp data, as detailed in this paper. The simulations further illustrate that the simple barrier model used to express the rate constants as a function of voltage is a reasonable approximation to the experimental data.

The voltage-dependent impedance functions observed in the presence of NMDA are indicative of a strong negative conductance that progresses with depolarization to a highly resonating system. The linear system is highly unstable and inverse transforms of the impedance functions show increasing oscillations with time. Since the system is highly non-linear, these oscillations are stable in the simulations, as would be expected in a real neuron. Fig. 8 illustrates stable oscillations for different levels of constant current injections as computed from equation 3.

Although there is evidence for membrane oscillatory processes during the locomotor cycle, a pure membrane origin for the potential oscillations during locomotion is unlikely since the principal drive for neural circuit behavior is synaptic in origin. Voltage-dependent phenomena, such as NMDA-induced membrane properties, are probably responsible for an amplification of EPSPs induced during small depolarizations. During NMDA-induced fictive locomotion, the membrane potential oscillations are clearly a complex mixture of both inherent membrane properties and synaptic drive. However, with NMDA-induced locomotion, it has been shown that the potential oscillations are similar to those seen during normal locomotion (Wallén and Grillner, 1987). Furthermore, a whole cell bathed in NMDA and showing oscillations in the presence of TTX provides a good model of the membrane properties likely to be involved at specific synaptic sites that are of the NMDA class.

References

ARMSTRONG, C. (1969). Inactivation of the potassium conductance and related phenomena caused by quarternary ammonium ion injected in squid axons. *J. gen. Physiol.* **54**, 553–575.

ASCHER, P. AND NOWAK, L.(1988). The role of divalent cations in the *N*-methyl-D-aspartate responses of mouse central neurones in culture. *J. Physiol., Lond.* **399**, 247–266.

AULT, B., EVANS, R. H., FRANCIS, A. A., OAKES, D. J. AND WATKINS, J. C. (1980). Selective depression of excitatory amino acid induced depolarizations by magnesium ions in isolated spinal cord preparations. *J. Physiol., Lond.* **307**, 413–428.

BRODIN, L., TRÅVÉN, H. G. G., LANSNER, A., WALLÉN, P., EKEBERG, Ö. AND GRILLNER, S. (1991). Computer simulations of *N*-methyl-D-aspartate receptor-induced membrane properties in a neuron model. *J. Neurophysiol.* **66**, 473–484.

BRODIN, L. AND GRILLNER, S. (1986). Effects of magnesium on fictive locomotion induced by activation of *N*-methyl-D-aspartate (NMDA) receptors in the lamprey spinal cord *in vitro*. *Brain Res.* **380**, 244–252.

BRODIN, L., TOSSMAN, U., OHTA, Y., UNGERSTEDT, U. AND GRILLNER, S.(1988). The effect of an uptake inhibitor (dihydrokainate) on endogenous excitatory amino acids in the lamprey spinal cord as revealed by microdialysis. *Brain Res.* **458**, 166–169.

BUCHANAN, J. T. (1986). Premotor interneurons in the lamprey spinal cord: morphology, synaptic interactions and activities during fictive swimming. In *Neurobiology of Vertebrate Locomotion* (ed. S. Grillner, P. S. G. Stein, D. G. Stuart, H. Forssberg and R. M. Herman), pp. 321–334. London: Macmillan

BUCHANAN, J. T., CHRISTENSEN, B. N. AND MOORE, L. E. (1989*a*). Amino acid responses of lamprey spinal neurons. *Soc. Neurosci. Abstr.* **15**, 1308.

BUCHANAN, J. T. AND GRILLNER, S. (1987). Newly identified glutamate interneurons and their role in locomotion in the lamprey spinal cord. *Science* **236**, 312–314.

BUCHANAN, J. T., GRILLNER, S., CULLHEIM, S. AND RISLING, M. (1989*b*). Identification of excitatory interneurons contributing to generation of locomotion in lamprey: structure, pharmacology and function. *J. Neurophysiol.* **62**, 59–69.

BUCHANAN, J. T., MOORE, L. E., HILL, R., WALLÉN, P. AND GRILLNER, S.(1992). Synaptic potentials and transfer functions of spinal neurons. *Biol. Cybernetics* **67**, 123–131.

DALE, N. AND GRILLNER, S. (1986). Dual-component synaptic potentials in the lamprey mediated by excitatory amino acid receptors. *J. Neurosci.* **6**, 2653–2661.

EKEBERG, Ö, WALLÉN, P., LANSNER, A., TRÅVEN, H., BRODIN, L. AND GRILLNER, S. (1991). A computer based model for realistic simulations of neural networks. I. The single neuron and synaptic interaction. *Biol. Cybernetics* **65**, 81–90.

FISHMAN, H. M., POUSSART, D. J. M., MOORE, L. E. AND SIEBENGA, E.(1977). K^+ conduction description from the low frequency impedance and admittance of squid axon. *J. Membr. Biol.* **32**, 255–290.

FLATMAN, J. A., SCHWINDT, P. C., CRILL, W. E. AND STAFSTROM, C. E. (1983). Multiple actions of *N*-methyl-D-aspartate on cat neocortical neurons *in vitro*. *Brain Res.* **266**, 169–173.

FRANKENHAEUSER, B. AND HUXLEY, A. F. (1964). The action potential in the myelinated nerve fibre of *Xenopus laevis* as computed on the basis of voltage clamp data. *J. Physiol., Lond.* **171**, 302–315.

GETTING, P. A. (1989). Emerging principles governing the operation of neural networks. *A. Rev. Neurosci.* **12**, 185–204.

GRILLNER, S., BRODIN, L., BUCHANAN, J. T., WALLÉN, P., DALE, N., HILL, R. AND MOORE, L. E. (1986). Excitatory amino acid neurotransmission in the lamprey spinal cord a key role in the generation of locomotion. In *Excitatory Amino Acid Transmitters* (ed. P. Hicks, D. Lodge and H. McLennan), pp. 293–300. New York: Alan Liss, Inc.

GRILLNER, S., BUCHANAN, J. T. AND LANSNER, A. (1988). Simulation of the segmental burst generating network for locomotion in lamprey. *Neurosci. Lett.* **89**, 31–35.

GRILLNER, S., MCCLELLAN, A., SIGVARDT, K., WALLÉN, P. AND WILN, M. (1981). Activation of NMDA-receptors elicits 'fictive' locomotion in lamprey spinal cord *in vitro*. *Acta physiol. scand.* **113**, 549–551.

GRILLNER, S. AND WALLÉN, P. (1985). The ionic mechansims underlying *N*-methyl-D-aspartate receptor-induced, tetrodotoxin-resistant membrane potential oscillations in lamprey neurons active during locomotion. *Neurosci. Lett.* **60**, 289–294.

GRILLNER, S., WALLÉN, P. AND BRODIN, L. (1991). Neuronal network generating locomotor behavior in lamprey: circuitry, transmitters, membrane properties and simulation. *A. Rev. Neurosci.* **14**, 169–199.

GRILLNER, S., WALLÉN, P., DALE, N., BRODIN, L., BUCHANAN, L. AND HILL, R. (1987). Transmitters, membrane properties and network circuitry in the control of locomotion in lamprey. *Trends Neurosci.* **10**, 34–41.

HILL, R. H., ÅRHEM, P. AND GRILLNER, S. (1985). Ionic mechanisms of three types of functionally different neurons in the lamprey spinal cord. *Brain Res.* **358**, 40–52.

HILL, R. H., BRODIN, L. AND GRILLNER, S. (1989). Activation of *N*-methyl-D-aspartate (NMDA) receptors augments repolarizing responses in lamprey spinal neurons. *Brain Res.* **499**, 388–392.

HODGKIN, A. L. AND HUXLEY, A. (1952). A quantitative description of membrane current and its application to conduction and excitation in nerve. *J. Physiol., Lond.* **117**, 500–544.

HOLMES, W. R. AND LEVY, W. B. (1990). Insights into associative long-term potentiation from computationsl models of NMDA receptor-mediated calcium influx and intracellular calcium concentration changes. *J. Neurophysiol.* **63**, 1148–1168.

HOMMA, S. AND ROVAINEN, C. M. (1978). Conductance increases produced by glycine and gamma-aminobutyric acid in lamprey interneurones. *J. Physiol., Lond.* **279**, 231–252.

JAHNSEN, H. AND LLINÀS, R.(1984). Ionic basis for the electro-responsiveness and oscillatory properties of guinea-pig thalamic neurones *in vitro*. *J. Physiol., Lond*. **349**, 227–247.

JAHR, C. E. AND STEVENS, C. F. (1987). Glutamate activated multiple single channel conductance in hippocampal neurons. *Nature* **325**, 522–525.

JAHR, C. E. AND STEVENS, C. F. (1990*a*). A quantitative description of NMDA receptor-channel kinetic behavior. *J. Neurosci* **10**, 1830–1837.

JAHR, C. E. AND STEVENS, C. F. (1990*b*). Voltage dependence of NMDA-activated macroscopic conductances predicted by single-channel kinetics. *J. Neurosc*. **10**, 3178–3182.

KOCH, C. (1984). Cable theory in neurons with active, linearized membranes. *Biol. Cybernetics* **50**, 15–33.

KOCH, C. AND SEGEV, I.(1989). *Methods in Neuronal Modeling.* Cambridge: MIT Press.

LLINÀS, R. AND YAROM, Y. (1986). Oscillatory properties of guinea-pig inferior olivary neurones and their pharmacological modulation: an *in vitro* study. *J. Physiol., Lond*. **376**, 163–182.

MACGREGOR, R. J.(1987). *Neural and Brain Modeling.* New York: Academic Press.

MARMARELIS, P. Z. AND MARMARELIS, V. Z.(1978). *Analysis of Physiological Systems. The White Noise Approach*. New York: Plenum.

MARTIN, A. R., WICKELGREN, W. O. AND BERANEK, R.(1970). Effects of iontophoretically applied drugs on spinal interneurones of the lamprey. *J. Physiol., Lond.* **207**, 653–665.

MAURO, A., CONTI, F., DODGE, F. AND SCHOR, R. (1970). Subthreshold behavior and phenomenological impedance of the squid giant axon. *J. gen. Physiol.* **55**, 497–523.

MAYER, M. L. AND WESTBROOK, G. L. (1985). The action of *N*-methyl-D-aspartic acid on mouse spinal neurones in culture. *J. Physiol., Lond.* **361**, 65–90.

MAYER, M. L. AND WESTBROOK, G. L.(1987). The physiology of excitatory amino acids in the vertebrate central nervous system. *Prog. Neurobiol.* **28**, 197–276.

MOORE, L. E. AND BUCHANAN, J. T. (1989). Synaptic transfer function of giant axon terminal–spinal neuron of the lamprey. *Neurosci. Soc. Abstr.* **516**, 6.

MOORE, L. E. AND CHRISTENSEN, B. N.(1985). White noise analysis of cable properties of neuroblastoma cells and lamprey central neurons. *J. Neurophysiol.* **53**, 636–651.

MOORE, L. E., HILL, R. H. AND GRILLNER, S.(1987). Voltage clamp analysis of lamprey neurons – role of *N*-methyl-D-aspartate receptors in fictive locomotion. *Brain Res.* **419**, 397–402.

MOORE, L. E., HILL, R. H. AND GRILLNER, S. (1993). Voltage clamp frequency domain analysis of NMDA activated neurons. *J. exp. Biol.* **175**, 59–87.

MOORE, L. E., YOSHII, K. AND CHRISTENSEN, B. N. (1988). Transfer impedances between different regions of branched excitable cells. *J. Neurophysiol.* **59**, 689–705.

MORRIS, C. AND LECAR, H.(1981). Voltage oscillations in the barnacle giant muscle fiber. *Biophys. J.* **35**, 193–213.

NOBLE, D. (1966). Applications of Hodgkin–Huxley equations to excitable tissues. *Physiol. Rev.* **46**, 1–50.

NOWAK, L., BREGETOVSKI, P., ASCHER, P., HERBET, A. AND PROCHIANTZ, A. (1984). Magnesium gates glutamate activated channels in mouse central neurones. *Nature* **307**, 462–465.

RASMUSSON, R. L., CLARK, J. W., GILES, W. R., ROBINSON, K., CLARK, R. B., SHIBATA, E. F. AND

CAMPBELL, D. L. (1990*a*). A mathematical model of the elecrophysiological activity in a bullfrog atrial cell. *Am. J. Physiol.* **259**, H370–H389.

RASMUSSON, R. L., CLARK, J. W., GILES, W. R., SHIBATA, E. F. AND CAMPBELL, D. L. (1990*b*). A mathematical model of a bullfrog cardiac pacemaker cell. *Am. J. Physiol.* **259**, H352–H369.

ROVAINEN, C. M. (1974). Synaptic interactions of identified nerve cells in the spinal cord of the sea lamprey. *J. comp. Neurol.* **154**, 189–206.

SAH, P., HESTRIN, S. AND NICOLL, R. A. (1989). Tonic activation of NMDA receptors by ambient glutamate enhances excitability of neurons. *Science* **246**, 815–818.

TRAUB, R. D. (1982). Simulation of intrinsic bursting in CA3 hippocampal neurons. *Neuroscience* **7**, 1233–1242.

WALLÉN, P. AND GRILLNER, S. (1987). *N*-Methyl-D-aspartate receptor-induced, inherent oscillatory activity in neurons active during fictive locomotion in the lamprey. *J. Neurosci*. **7**, 2745–2755.

WATKINS, J. C. AND OLVERMAN, H. J. (1987). Agonists and antagonists for excitatory amino acid receptors. *Trends Neurosci.* **10**, 265–272